GNNs for Multi-Region Neural Silence Detection

Diksha Agarwal* and Dr. Alireza Chamanzar†

***Abstract*—Identifying neural silences is critical to understanding brain function and dysfunction. We present a Graph Neural Network (GNN) framework that encodes EEG channels as feature vectors comprising binary beta, squared beta, and graph node degree, capturing both source-level brain activity and connectivity information to detect multiple silent regions. Our method analyzes regions of silence across both hemispheres and achieves accurate multi-region localization with a mean Jaccard index of 0.79 and mean center-of-mass error of 2.19 mm, outperforming baseline approaches. This approach enables rapid, noninvasive mapping of complex silent patterns, highlighting the potential of graph-based deep learning for scalable brain monitoring.**

***Index Terms*—GNN, Jaccard index, center-of-mass, beta**

I. Introduction

Understanding neural activity, including regions that are silent or minimally active, is critical for deciphering brain function. Neural silences—areas with little or no electrophysiological activity—are associated with cognitive states, development, and neurological disorders. Accurate localization of these regions provides insights for both neuroscience and clinical applications, such as monitoring recovery after cortical resection or identifying pathological areas.

Current methods for detecting silent regions are often resource-intensive and limited to single-region analysis, restricting their accessibility. Developing a cost-effective, noninvasive approach capable of localizing multiple silent regions can expand advanced brain monitoring to rural or resource-limited settings, improving care for underserved populations.

Prior work has shown that noninvasive scalp EEG can detect single regions of neural silence. For example, [1] introduced SilenceMap, which combines EEG measurements with baseline normalization and spectral clustering to estimate silent regions.

In this work, we present a GNN-based framework for multi-region neural silence localization. By representing EEG channels as feature vectors encoding both signal and connectivity information, the GNN captures patterns indicative of cortical silence. Evaluations on simulated data demonstrate improved accuracy and robustness over conventional methods, representing a significant step toward fast, noninvasive, and scalable mapping of complex neural silence patterns in the human brain.

II. SilenceMap Optimization Framework

Following standard source localization, neural activity and resulting scalp potentials are modeled via a linear forward model derived from Poisson's equation:

$$\mathbf{X}_{n\times T} = \mathbf{A}_{n\times p}\,\mathbf{S}_{p\times T} + \mathbf{E}_{n\times T}, \tag{1}$$

where $\mathbf{A}$ is the forward matrix, $\mathbf{X}$ the recorded scalp potentials, $\mathbf{S}$ the source signals, $\mathbf{E}$ measurement noise, n electrodes, p sources, and T time samples.

Only differential scalp potentials are measurable. Let $\mathbf{M}_{(n-1)\times n}$ be a differential operator with its last column -1 and first $(n-1)$ columns as identity. Then

$$\mathbf{Y}_{(n-1)\times T} = \mathbf{M}_{(n-1)\times n}\,\mathbf{A}_{n\times p}\,\mathbf{S}_{p\times T} + \mathbf{M}_{(n-1)\times n}\,\mathbf{E}_{n\times T}. \tag{2}$$

This can be rewritten compactly as

$$\mathbf{Y} = \widetilde{\mathbf{A}}\,\mathbf{S} + \widetilde{\mathbf{E}}, \tag{3}$$

where $\widetilde{\mathbf{A}} = \mathbf{MA}$ and $\widetilde{\mathbf{E}} = \mathbf{ME}$.

We assume that some sources exhibit *stationary regions of silence*, where $s_i(t) = 0$ for contiguous time segments. All sources are silent simultaneously. Each zero-valued segment defines a *region of silence*, and the corresponding row indices indicate its location. The total number of such rows or contiguous groups determines the *number of regions of silence* in the system.

Note: This work uses simulated EEG data, which does not include a reference electrode (M). The proposed GNN framework is compatible with real EEG recordings where signals are measured relative to a reference electrode.

III. Definition of Silence Regions

For each source $i \in \{1, 2, \ldots, p\}$, define the silence indicator

$$z_i = \begin{cases} 0, & \text{if } s_i(t) = 0,\ \forall t \in [1, T], \\ 1, & \text{otherwise.} \end{cases} \tag{4}$$

Then, the binary vector $\mathbf{z} = [z_1, z_2, \ldots, z_p]^\top$ encodes the spatial pattern of silence across sources. Regions of silence are formed by contiguous sequences of zero-valued entries in $\mathbf{z}$.

Formally, the r^{th} region of silence is defined as

$$\mathcal{R}_r = \{\, i \mid z_i = 0,\ i \in [a_r, b_r] \,\}, \tag{5}$$

where a_r and b_r are the indices of the first and last silent sources in that contiguous segment. The total number of distinct silence regions is

$$R = |\{\, \mathcal{R}_1, \mathcal{R}_2, \ldots, \mathcal{R}_R \,\}|. \tag{6}$$

Example

Consider an example with $p = 4$ sources and $T = 4$ time samples:

$$\mathbf{S} = \begin{bmatrix} 0 & 0 & 0 & 0 \\ 1 & 2 & 3 & 2 \\ 0 & 0 & 0 & 0 \\ 0 & 0 & 0 & 0 \end{bmatrix}.$$

Here, sources 1, 3, and 4 are completely silent, while source 2 is active. Grouping contiguous silent rows yields

$$\mathcal{R}_1 = \{1\}, \quad \mathcal{R}_2 = \{3, 4\},$$

and thus the total number of silence regions is $R = 2$.

Objective

The goal is to automatically determine:

1) The indices of sources belonging to each region of silence $\mathcal{R}_r$, and
2) The total number of distinct silence regions R.

IV. Assumptions

We make the following assumptions:

1) The matrices $\mathbf{A}$ and $\mathbf{M}$ are known, and $\mathbf{Y}$ is measured.
2) Noise $\widetilde{\mathbf{E}}$ is an additive white noise, whose elements are assumed to be independent in the space.

$$c_{z_{ij}} = \begin{cases} \sigma_{z_i}^2, & i = j, \\ 0, & i \neq j. \end{cases}$$

where $\sigma_{z_i}^2$ is the noise variance at the electrode i, and it is assumed to be known.

3) Now suppose there are K silent regions: S_1,S_2,..., S_K and we don't know K. But the regions themselves are separated in space. The rest of the brain (the complement) remains active and correlated.
4) Covariance structure for multiple silent regions
When extending the model to allow multiple stationary regions of silence, the source covariance matrix $\mathbf{C}_s$ becomes *block-structured*. Let $\{S_1, S_2, \dots, S_K\}$ denote K disjoint silent regions, each representing a spatially contiguous cluster of inactive sources. Then the covariance between sources i and j is defined as

$$(\mathbf{C}_s)_{ij} = \begin{cases} \sigma_s^2 \exp\Big(-\gamma \,\|\mathbf{f}_i - \mathbf{f}_j\|^2\Big), & \text{if } i, j \notin \bigcup_{k=1}^{K} S_k \\ 0, & \text{if } i \in S_k \text{ or } j \in S_k, \\ & \text{for any } k \end{cases} \tag{7}$$

where σ_s^2 is the source variance, γ controls the spatial decay of correlation, and $\mathbf{f}_i \in \mathbb{R}^3$ denotes the 3D position of source i on the cortical surface.

a) Interpretation.: This formulation implies that any source belonging to a silent region contributes no variance (its diagonal entry is zero), and all cross-covariances involving that source are also zeroed out. Only sources outside the union of all silent regions remain correlated through the exponential spatial kernel. Therefore, instead of a single contiguous zero block as in the single-region case, $\mathbf{C}_s$ now exhibits multiple scattered zero blocks, each corresponding to one distinct silent region.

5) M is a matrix $(n-1) \times n$ where the last column is $(-1)_{(n-1)\times 1}$ and the first n - 1 columns form an identity matrix $(I)_{(n-1)\times(n-1)}$.
6) We assume that $p - k_{\text{silent}} \gg k_{\text{silent}}$, where $(p - k_{\text{silent}})$ denotes the number of active sources and k_{silent} denotes the number of silent sources.
7) Definition of contiguity. Silent sources are assumed to form *contiguous regions* on the cortical surface. We define contiguity based on a z-nearest neighbor (z-NN) graph, where the nodes correspond to brain sources (i.e., vertices in the discretized cortical model). In this z-nearest neighbor graph, two nodes i and j are connected with an edge if either or both of them is among the z nearest neighbors of the other node, where z is a known hyperparameter controlling local connectivity.
A *contiguous region of silence* is then defined as any *connected subgraph* of this z-nearest neighbor graph. That is, for any pair of nodes within the region, there exists at least one connecting path that lies entirely within the region. Each connected subgraph thus represents a spatially coherent cluster of silent sources. In our model, we allow for multiple distinct regions of silence on the cortical surface. These regions are defined with respect to the z-nearest neighbor graph $G = (V, E)$, where each node in $V = \{1, \dots, p\}$ represents a cortical source, and edges in E connect spatially adjacent sources.
Let $\mathcal{R}_1, \mathcal{R}_2, \dots, \mathcal{R}_K$ denote the sets of silent sources. Each $\mathcal{R}_k$ corresponds to a *connected subgraph* of G, meaning that for any two nodes $i, j \in \mathcal{R}_k$, there exists at least one path between them that lies entirely within $\mathcal{R}_k$. Different silent regions are *disjoint*, i.e.,

$$\mathcal{R}_i \cap \mathcal{R}_j = \emptyset, \quad \forall i \neq j,$$

ensuring that the silent regions do not spatially overlap. Thus, the silent sources decompose into K connected components on the underlying cortical graph.

8) The S vector has no temporal bounds.
9) We assume that region of silence can be in any hemisphere.
10) We have assumed S_1, S_2 to be disjoint. So no overlap is considered.

V. PROPOSED ALGORITHM

A. Real Forward Model Loading

We use a realistic head model consisting of a leadfield matrix $L \in \mathbb{R}^{n\times p}$ and cortical surface coordinates $X \in \mathbb{R}^{p\times 3}$.

B. Silent Region Definition on the Real Cortex

Silent regions are constructed directly on the real cortical surface. To avoid midline ambiguity, vertices satisfying $|x_i| < 5\,\mathrm{mm}$ are excluded from selection as centers of the silent-region.

We generate K spatially compact regions. For each region, a center vertex is chosen from the remaining allowed set. Distances from the center to all other vertices are computed, and the closest k_{reg} neighbours form one silent region. Selected vertices are removed to prevent region overlap.

The resulting ground-truth silent mask is:

$$X_{\text{act}}[i] = \begin{cases} 0, & \text{if node } i \text{ is silent,} \\ 1, & \text{otherwise.} \end{cases}$$

C. EEG Simulation Using Real Leadfield

D. Computation of the Activity Proxy β

- **Binary** β is input to GNN

E. Self-Supervised GNN Using a Single β

Graph Setup

- We reuse the cortical graph and build a normalized adjacency matrix:

$$\tilde{A}_{ij} = \frac{W_{ij}}{\sqrt{d_i d_j}}.$$

- Each node receives a 3-dimensional feature vector:

$$x_i = (\beta_i,\ \beta_i^2,\ d_i).$$

GNN Architecture

- Input layer: maps the 3 features into a hidden space.
- Two message-passing layers:
  - one using 1-hop neighbors,
  - one using 2-hop neighbors.
- Output layer: uses `softplus` to keep all outputs non-negative.

Self-Supervised Loss

The total loss has three terms:

$$L = L_{\text{data}} + \lambda_{\text{gnn}} L_{\text{smooth}} + \gamma_{\text{gnn}} L_{\text{seed}}.$$

- **Data term:**

$$L_{\text{data}} = \|g - \beta\|_2^2$$

  makes the prediction close to the measured vector β.
- **Smoothness term:**

$$L_{\text{smooth}} = g^\top L g$$

  encourages nearby nodes to have similar values.
- **Seed term:**

$$L_{\text{seed}} = \frac{1}{|S_{\text{seed}}|} \sum_{i \in S_{\text{seed}}} g_i$$

  pushes nodes with very low β values (the seeds) toward zero.

Key Idea

- No labels are needed.
- The GNN learns from a single β vector using:
  - the graph structure (Laplacian),
  - the assumption that lowest β values indicate silent regions.

Final Output

- After training, the GNN output g_{gnn} is normalized to $[0, 1]$.
- We threshold the lowest q_{silent} percent to detect silent regions.

The cortical graph is reused to construct the normalized adjacency:

$$\widehat{A}_{ij} = \frac{W_{ij}}{\sqrt{d_i d_j}}.$$

Each vertex receives the feature vector:

$$x_i = (\beta_i, \beta_i^2, d_i).$$

The GNN consists of:

- an input encoder mapping $\mathbb{R}^3 \to \mathbb{R}^h$,
- two message-passing layers using 1-hop and 2-hop diffusion,
- a non-negative output layer using $\mathrm{softplus}(\cdot)$.

The self-supervised loss contains three terms:

$$\mathcal{L} = \underbrace{\|g - \beta\|_2^2}_{\mathcal{L}_{\text{data}}} + \underbrace{\lambda_{\text{gnn}}\, g^\top L_g g}_{\mathcal{L}_{\text{smooth}}} + \underbrace{\gamma_{\text{gnn}} \frac{1}{|S_{\text{seed}}|} \sum_{i \in S_{\text{seed}}} g_i}_{\mathcal{L}_{\text{seed}}},$$

where S_{seed} is the set of nodes whose β falls within the lowest $q_{\text{silent}}\%$.

Unlike supervised methods, the GNN requires no labels and learns from a *single* β vector using the Laplacian geometry and seed suppression.

After training, g_{gnn} is normalized to $[0, 1]$ and thresholded at the same percentile q_{silent} to predict silent regions.

VI. Results

The results are as follows where Fig 1 indicates Simulated Ground Truth **(in this case all region of silence lies in single hemisphere)**, Fig 2 indicates GNN predicted regions of silence and Fig 3 represents clusters marked with the scoring mechanism used. Here K = number of regions of silence. In experiment we consider K = 5, q represents percentage of cortex covered. We keep 50 nodes as silent from 1662 nodes. Also, created a comparative study in Fig 4 between ground truth, GNN and clusters to visualize clusters from different angles. In Fig 4 we have considered testcase where **(region of silence lies in both hemisphere)**
Clusters of silent nodes were ranked using a score defined as:

$$\text{Score} = \frac{\text{size}}{\text{radius}} \tag{8}$$

where *size* is the number of nodes in the cluster, *radius* is the median Euclidean distance of nodes from the cluster centroid, and *centroid* is the mean of detected coordinates within a cluster.

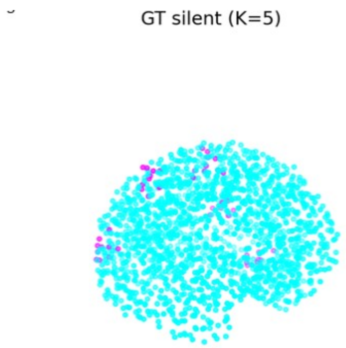

Fig. 1. Ground Truth silence regions.

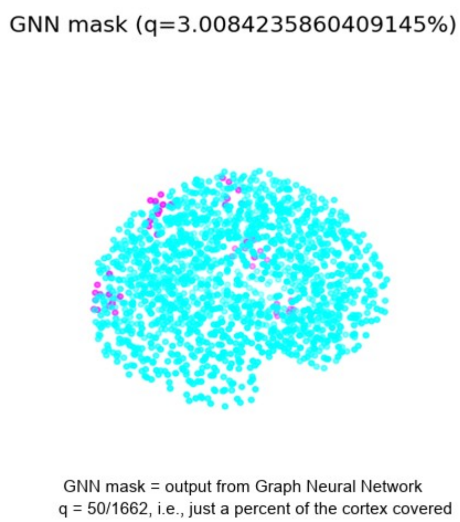

Fig. 2. GNN-predicted silence map.

A. GNN Cluster Analysis for Fig. 3

Table I shows the detected GNN clusters and their properties, including size, radius, and cluster score.

TABLE I
DETECTED GNN CLUSTERS AND THEIR PROPERTIES (FIG. 3)

Rank	Cluster ID	Size	Radius	Score
0	C2	13	8.78	1.481
1	C4	12	9.51	1.261
2	C3	10	8.63	1.159
3	C1	9	8.45	1.065
4	C0	6	8.74	0.687

Evaluation Metrics: The following metrics were computed for the predicted clusters:

- Mean Jaccard Index: 0.784

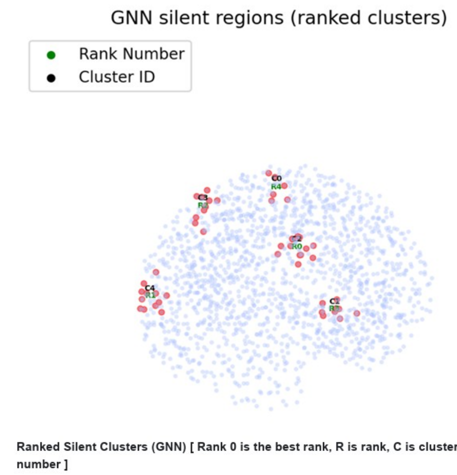

Fig. 3. Cluster ranking output.

- Mean ΔCOM: 2.121 mm
- Mean size relative error (Δk): 0.200

Cluster-to-Ground Truth Matching: Table II shows the correspondence between predicted clusters and ground truth.

TABLE II
COMPARISON OF PREDICTED CLUSTERS TO GROUND TRUTH (FIG. 3)

GT	Pred	Jaccard	ΔCOM (mm)	Size GT	Size Pred
G2	C2	0.769	2.43	10	13
G0	C0	0.600	2.78	10	6
G4	C4	0.833	1.71	10	12
G3	C3	0.818	2.20	10	10
G1	C1	0.900	1.50	10	9

These results indicate that the GNN model captures the spatial structure of the silence regions with high consistency, achieving strong overlap (Jaccard $\approx$ 0.78), small localization error (ΔCOM $\approx$ 2.12 mm), and low size deviation.

B. GNN Cluster Analysis for Fig. 4

In case, of Fig 4 the case where region of silence lies in both hemisphere the results are as follows:

GNN Cluster Properties: The GNN identified 5 clusters among silent nodes. Table III summarizes the properties and ranking of each cluster.

TABLE III
GNN CLUSTER PROPERTIES AND SCORES

Rank	Cluster	Size	Radius	Score
0	C1	14	9.33	1.501
1	C2	10	7.29	1.372
2	C4	12	11.01	1.090
3	C3	7	7.63	0.917
4	C0	7	8.56	0.818

Evaluation Against Ground Truth: Table IV shows the cluster-to-ground truth correspondence. We report the **Jaccard index** (J), center-of-mass error (ΔCOM), and cluster sizes for both ground truth and predicted clusters.

TABLE IV
CLUSTER-TO-GROUND TRUTH MATCHING

GT	Pred	Jaccard	ΔCOM (mm)	Size GT	Size Pred
G2	C2	1.000	0.00	10	10
G1	C1	0.714	2.03	10	14
G3	C3	0.700	3.08	10	7
G4	C4	0.833	2.71	10	12
G0	C0	0.700	3.13	10	7

Evaluation Metrics: The mean evaluation metrics are as follows:

- Mean Jaccard index: 0.790
- Mean center-of-mass error (ΔCOM): 2.19 mm
- Mean relative size error (Δk): 0.24

These results indicate that the GNN accurately identifies silent regions, achieving high overlap with ground truth clusters while maintaining close centroid alignment. Clusters with perfect Jaccard scores (e.g., G2 $\leftrightarrow$ C2) demonstrate exact recovery, whereas minor size discrepancies reflect the flexible nature of the GNN clustering.

VII. CONCLUSIONS

We propose a graph-based framework for detecting multiple regions of neural silence. By leveraging the spatial structure of the cortical surface and learning complex dependencies via GNNs, our method:

- Accurately identifies multiple silent regions
- Handles binary data and multi hemispheres region of silence
- Does not require labeled data

VIII. FUTURE WORK

Potential extensions include:

- Simulate non-binary beta
- Incorporating temporal dynamics to track evolving silence regions
- Adapting the GNN for fMRI and real EEG data.
- Exploring hierarchical GNNs for multi-scale silent region detection
- Extending to patient-specific or population-level studies

CODE AVAILABILITY

The code and data used in this work are available at https://drive.google.com/drive/folders/1AsSw6Y6aN09TIoyQAXNokZhZFGNkaRa0?usp=sharing

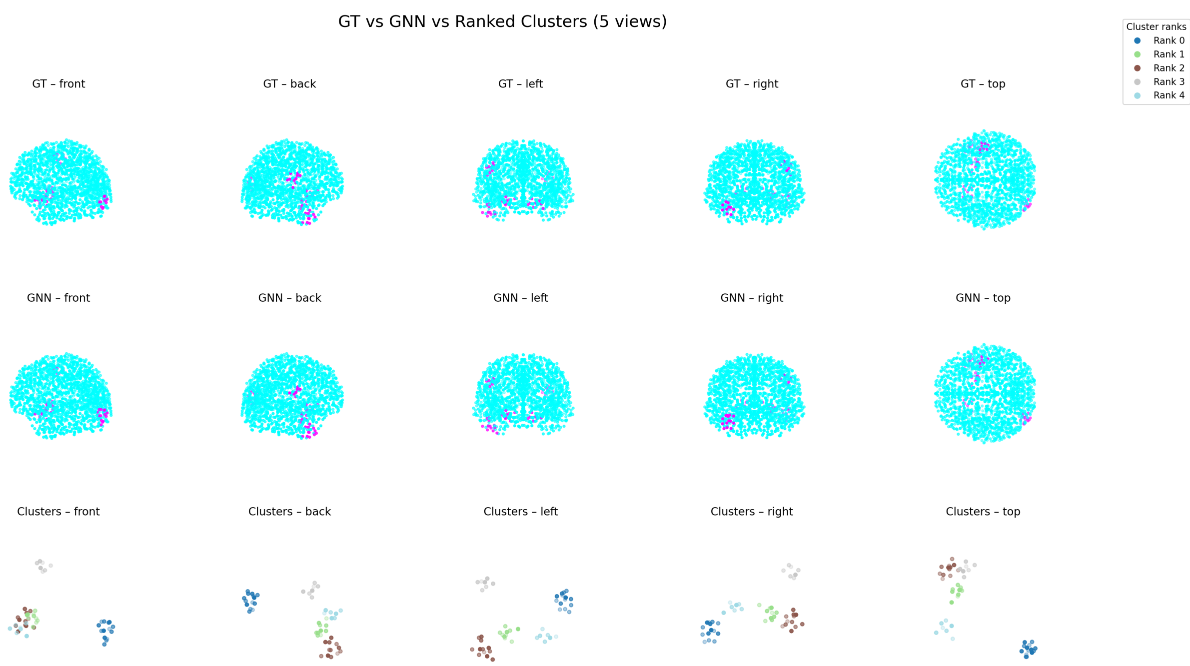

Fig. 4. Comparison between Ground Truth, GNN, and clusters, considering region of silence in both hemisphere of brain

References

[1] A. Chamanzar, M. Behrmann, and P. Grover, "Neural silences can be localized rapidly using noninvasive scalp eeg," *Communications biology*, vol. 4, no. 1, p. 429, 2021.